Magazine of Concrete Research
Volume 64 Issue 10

Economic design of beams with FRP rebar or prestress
Balafas and Burgoyne

Magazine of Concrete Research, 2012, **64**(10), 885–898
http://dx.doi.org/10.1680/macr.11.00099
Paper 1100099
Received 15/06/2011; revised 15/01/2012; accepted 17/02/2012

ice
Institution of Civil Engineers
publishing

Economic design of beams with FRP rebar or prestress

Ioannis Balafas
Department of Civil and Environmental Engineering, University of Cyprus, Nicosia, Cyprus

Chris J. Burgoyne
Department of Engineering, University of Cambridge, Cambridge, UK

Fibre-reinforced polymers (FRPs) have not captured the market for reinforcing bars, or found uses even as external prestressing tendons, despite their obvious advantages in terms of lack of corrosion. This paper considers the constraints that underlie the optimal design for beams reinforced or prestressed with FRP, and compares the result with designs for beams with steel reinforcement. This is done by means of a diagram that compares the depth of the beam with the area of reinforcement, on which most of the governing constraints can be plotted. The method allows generic conclusions to be drawn about the governing principles.

Introduction

When high-strength fibres (glass, aramid and carbon) were first introduced to the structural engineering world it was assumed that they would be most suitable for use as prestressing tendons, which are the most highly stressed of all structural elements: this would make maximum use of the high strength that was being provided so expensively. It was considered that use as reinforcement would seldom be justified, since deflections would govern and the fibres would rarely be stressed to a high load. Experience has shown, however, that there have been few applications of prestressing, despite the added benefit that fibre-reinforced polymer (FRP) tendons can be placed externally, and the limited use that has been made as reinforcement has been using glass-fibre-reinforced polymer (GFRP), which has the lowest stiffness and is thus more lightly stressed than aramid-fibre-reinforced polymer (AFRP) or carbon-fibre-reinforced polymer (CFRP) bars would be. This paper seeks to produce some general principles that explain why this might be the case.

The close fit between the strain capacities of steel and concrete means that they are ideally suited to produce a composite reinforced concrete where both materials are used economically, while strains and curvatures remain small. Steel is relatively cheap (aramid and carbon cost five to six times as much per unit of force), but corrosion of steel in concrete bridges is a major problem (Fickelhorn, 1990; Makhtouf *et al.*, 1991); by now FRPs should be in widespread use (Balafas, 2003). However, applications of FRP are still scarce; the market is hesitant to adopt them, partly because of their high cost and partly because the design principles differ from those using conventional rebar.

This paper addresses the question of how, or even whether, their properties should be included in the design process. The target is to identify ways in which FRP can be used at minimum cost, and to consider why FRPs are rarely used in practice. These questions will be addressed through the use of a diagram of depth (d) plotted against flexural bar area (A_p).

The first sections below will show how the basic diagrams are built up. Additional constraints will then be added before specific questions are answered about the different options available to designers. Three case studies will be considered before final conclusions are drawn.

Depth plotted against area diagram

The parameters affecting a design can be shown on a diagram of flexural bar area (A_p) against section depth (d), which was first introduced by Al-Salloum and Siddiqi (1994) for the optimal design of rectangular reinforced concrete beams. They considered only a limited number of design constraints. The method will be expanded here to include many different factors.

Detailed equations are not given below since the analysis follows standard procedures for the design of a cross-section on the assumption that plane sections remain plane. Safety factors are included for ultimate loads, but not for serviceability conditions. Sections are designed from first principles, rather than a particular code of practice, although some use is made of factors that are also used in codes. Very similar plots would result from using codes, and a detailed discussion of the differences would distract from the main argument. For the same reason, although all the plots below relate to the same loading case (see later Tables 3, 4 and 5), and have been produced as a result of specific calculations, details are not given here. Any beam design would result in similar plots that would only differ in minor details.

The following sections show how the basic diagram is built up.

Ultimate strength condition

The ultimate strength condition divides the d–A_p diagram into two zones (Figure 1(a)); sections that are sufficiently strong lie

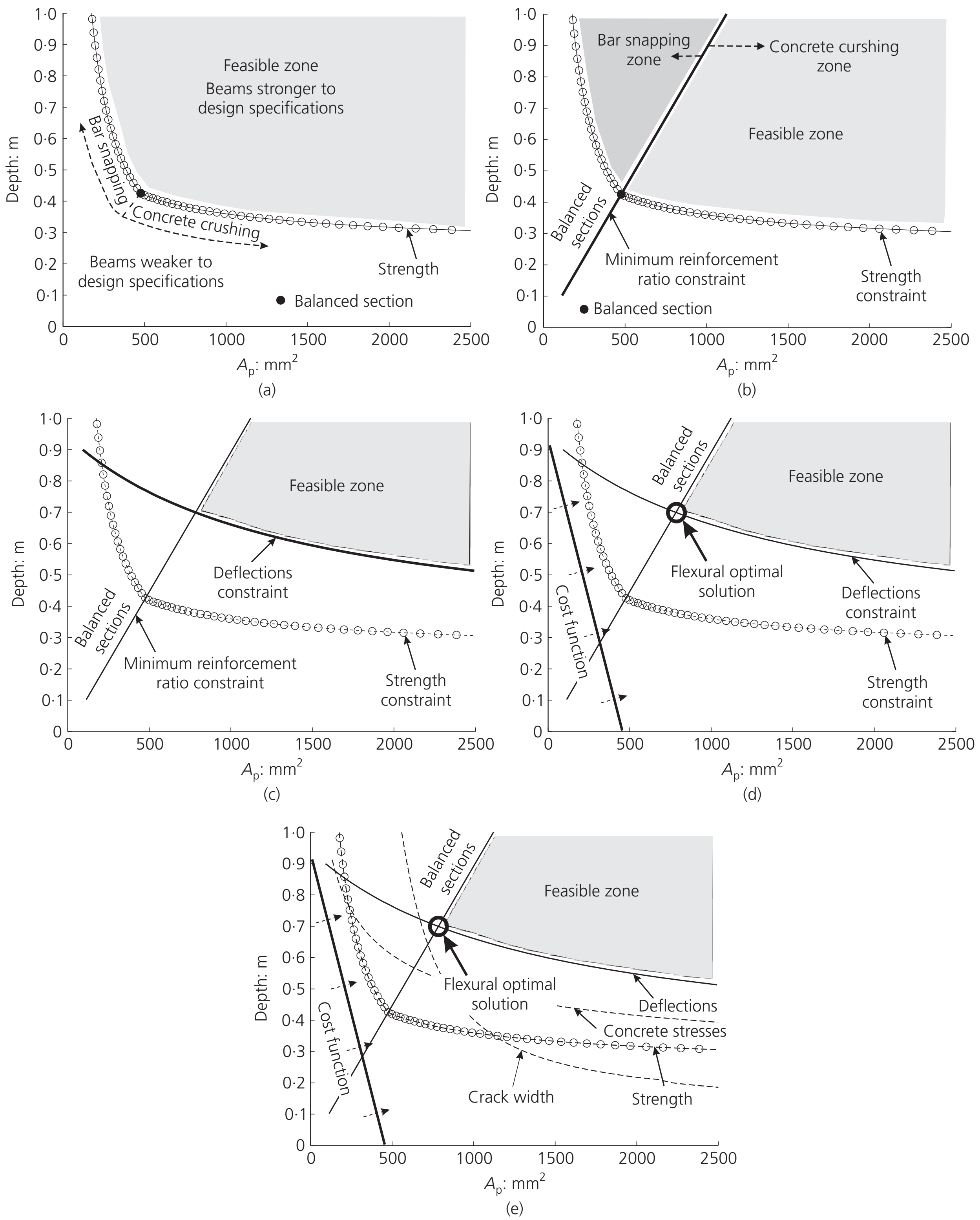

Figure 1. Depth against Ap diagram for reinforced concrete sections: (a) ultimate strength condition; (b) bar snapping condition; (c) deflection constraint; (d) cost function; (e) complete diagram for FRP-reinforced section

above a boundary line while those that are inadequate lie below it. The boundary line is curved and there is a distinct change in slope when the limiting condition changes from failure by tendon snapping to failure by concrete crushing.

Bar snapping condition

Unlike sections reinforced with steel that can yield, sections with FRP should not be allowed to fail by reinforcement snapping, so a minimum limit on the amount of reinforcement has to be applied that reduces the size of the feasible zone (Figure 1(b)). This will be referred to hereafter as the 'balanced-section' constraint. It could be argued that this limit only applies if the section were limited by strength criteria, as it is not relevant if the beam is deflection-limited, but it is argued here that the section should be proportioned in such a way that brittle failure is avoided even if the structure is overloaded.

Deflection condition

Sections with FRP reinforcement are more flexible than sections with steel rebar, so the deflection condition needs to be checked, which leads to a further reduction in the size of the feasible zone, as shown in Figure 1(c).

Cost function

The cost of the beam can be directly related to the cross-sectional area and the amount of reinforcement. Allowances can be made for the cost of the formwork, as well as for the shear reinforcement. Beams of equal cost are defined by a line of fixed slope on the d–A_p diagram; as the cost of the beam increases, this line moves to the right but the slope remains the same (Figure 1(d)). The optimum solution is therefore where the cost function line first meets the feasible region; in the example shown in Figure 1 that occurs when the bar snapping and deflection constraints meet.

Other constraints

Other constraints can also be shown. Crack-width limits can be introduced; for FRP-reinforced structures these are associated with appearance, while for steel-reinforced structures they are associated with durability. A limit on concrete stress, to eliminate the possibility of excessive creep, can also be considered. The latter rarely governs, but Figure 1(e) shows that the crack width is close to the limit for the cheapest design, in this particular case, and it can limit other cases.

The method does not specifically include the breadth of the beam. Only rarely is the breadth a governing condition; it will be assumed here that it is as small as practicable. The breadth does affect the amount of shear steel needed, and is reflected in the costs functions, but the details do not affect the main argument and will not be discussed further.

Applications of the d–A_p diagram

Having derived the basic diagram, it is now possible to compare different alternative designs. This will be done by showing pairs of diagrams for different cases, which allows the distinctions to be highlighted.

Steel against FRP

The most fundamental consideration when designing a reinforced concrete section is the choice of reinforcement material. To date, steel has been the obvious solution, and the d–A_p diagrams show why.

Figure 2 compares two designs (for the same loading case), one with steel rebar and one with FRP. A number of differences can be noted in the way the constraints apply.

(*a*) In the steel diagram, the strength condition is more critical than the deflection condition, except for very shallow beams.
(*b*) There are minimum areas of steel reinforcement (to avoid snapping or excessive cracking) as well as maximum areas (to avoid over-reinforcement).

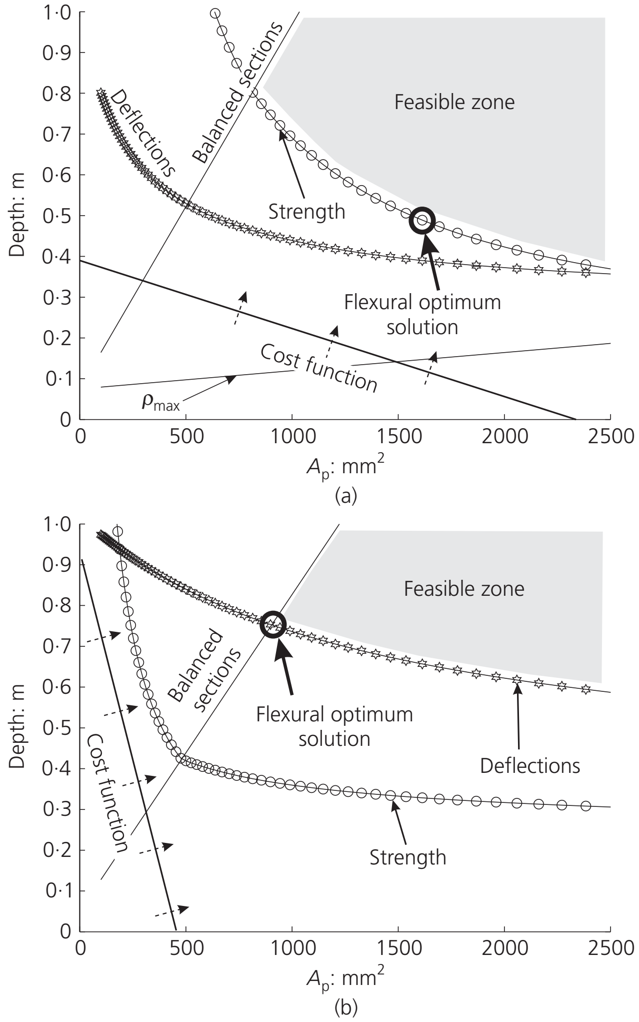

Figure 2. Beam with: (a) steel rebar; (b) FRP rebar

(*c*) Steel is much cheaper (per unit volume) than FRP, so the constant cost line is much flatter.
(*d*) The optimal design for use with FRP is almost always at the vertex where the deflection (or occasionally the crack width) conditions meet the deflection limit.
(*e*) The flexural optimum solution for steel reinforcement is not at a vertex but lies on a curved edge. There will thus be a range of designs that have very similar costs and the optimum design will be very sensitive to variations in the relative costs of labour and materials. This can mean that the optimum solution can alter depending on where the structure is built.

Furthermore, some conclusions can be drawn about the differences between the design with FRP and that with steel. Beams with FRP need to be significantly deeper than beams with steel in order to comply with the deflection conditions, but the amount of reinforcement required is less because the rebar is stronger.

Prestressed concrete beams

Prestressed concrete beams can be studied using the same basic principles, but different parameters become important. The most significant difference is the addition of upper and lower bounds on the section stresses at the working load. This has the corollary that there is an upper limit on the amount of prestress that can be applied, so the feasible zone is now bounded.

Stress rupture of FRP tendons also has to be considered, but it appears in these diagrams indirectly since it affects the allowable stress in the tendon, which in turn affects the A_p required.

Typical results are shown in Figure 3, (a) (for steel) and (b) for FRP. As with the plots for reinforced concrete design, the optimal design for sections with FRP is usually at a vertex of the feasible zone (which makes it relatively insensitive to changes in relative costs of reinforcement and concrete), while the optimum for a section prestressed with steel lies along a curved edge of the zone.

Deflection criteria are unlikely to govern for either material; the prestress prevents the section cracking at the working load so the beam stiffness is now almost entirely a property of the concrete and not of the reinforcement, even for sections prestressed with FRP.

Comparison of the two plots for prestressed beams yields conclusions that differ from those for reinforced sections. The optimum depth for both sections is similar, which is logical given that prestressing allows the concrete itself to carry the load. Less material is needed for prestressing with FRP because those tendons are generally stronger, while the stress-rupture and ultimate strength of the tendon enter by way of the balanced section criterion.

Case studies

The plots developed above are interesting in their own right, but having set out the basic principles of how the diagrams are produced, their use can be extended into a study which can map the design space and identify factors that most affect the economics of design. Three cases will be considered in more detail: a reinforced concrete beam and two prestressed concrete beams, one prestressed, the other statically indeterminate.

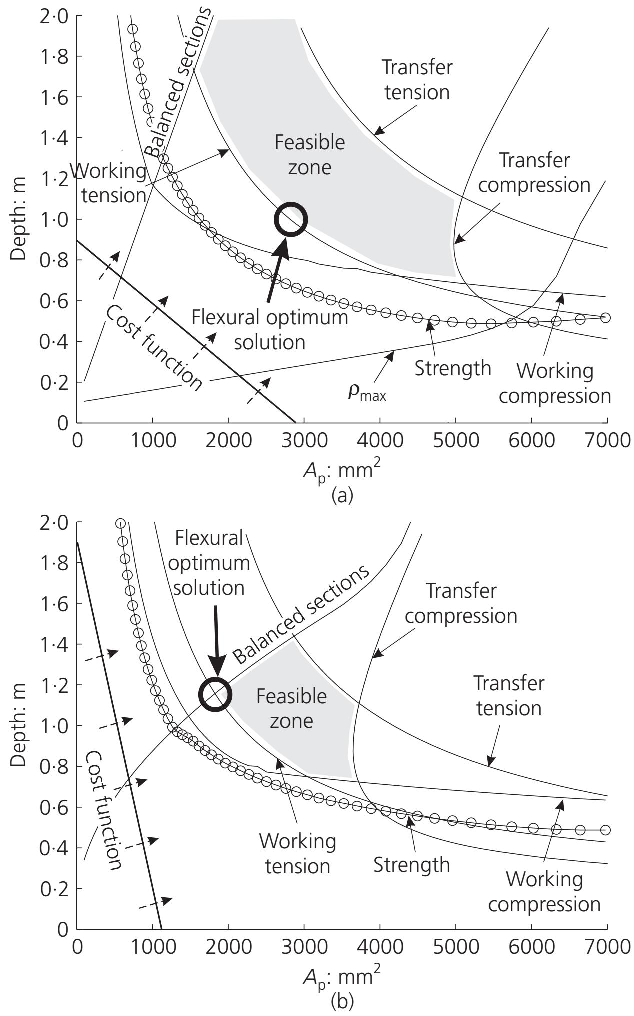

Figure 3. Beam with: (a) steel tendon; (b) FRP tendon

Materials considered in the case studies

Various FRP materials have been considered in this study. GFRP and CFRP are typically used in the form of pultruded rods of various diameters. Aramid fibres are available in various forms. Kevlar and Twaron fibres have very similar properties and are available in standard modulus and high modulus versions. The high modulus version is used in FiBRA, which is a braided product embedded in resin. The standard modulus version of a similar, but not identical product, Technora, is used to make a pultruded rod that is stronger but less stiff than the FiBRA. As aramid fibres are tougher than carbon, they can also be used without resin and are used as parallel-lay ropes under the name Parafil. These ropes can be fitted with termination systems that make them suitable for use as prestressing tendons, but they are not suitable for use as rebar.

Typical values for the strength and stiffness are given in Table 1. Under long-term loading strength may reduce owing to creep rupture; the strength at time t, f_t, is given by

$$f_t = f_i(1 - B \log_{10} t) \quad (1)$$

where f_i is the short-term strength, B is a constant determined by fitting to existing creep rupture data (Giannopoulos and Burgoyne, 2009; Yamaguchi *et al.*, 1998) and its values are shown in Table 1. Note that t is in hours. Creep rupture for steel is insignificant and thus ignored.

The unit costs for the different materials, obtained from recent quotations from manufacturers, are shown in Table 2. With these general values as a basis, it is now possible to investigate the effect of changing various aspects of the design.

Material	€/m³	€/kN/m
Concrete[a,b]: f_c in N/mm²	$48{\cdot}145e^{0{\cdot}0178 f_c}$	
Steel reinforcement[a,b]	6700	0·015
Steel tendon[a,b]	20 000	0·012
GFRP[c,d,e]	11 500	0·010
FiBRA[f]	82 000	0·055
Technora – Parafil[f]	82 000	0·043
CFRP bars[c,d,e]	90 000	0·041
Formwork[a,b]: €/m²	11	

[a] (Kallitsis O.E. Athens (2008) Personal communication), [b] (Republic of Cyprus – Ministry of Public Works (2008) Personal communication), [b] (Hughes Brothers, Inc. (2008) Personal communication), [d] (Pultrall, Inc. (2008) Personal communication), [e] (Sireg SpA (2008) Personal communication), [f](Linear Composites Limited (2008) Personal communication)

Table 2. Material costs

Case study 1. Reinforced concrete

The example chosen is a simply supported T-beam as shown in Figure 4. Several input parameters assumed in the analysis are shown in Table 3. The width of the web is assumed to be 250 mm. The beam and the slab are rigidly connected so the beam's cross-section is T-shaped. The effective width of the slab that acts compositely with the beam is difficult to determine. The normal calculations used in codes of practice (which typically give effective breadths = span/5) are designed to give a beam with an effective value of second moment of area, but the present analysis is more concerned with the peak compressive stress, which gives lower effective breadth (Hambly, 1991). The value used in this analysis is span/7 = 0·85 m.

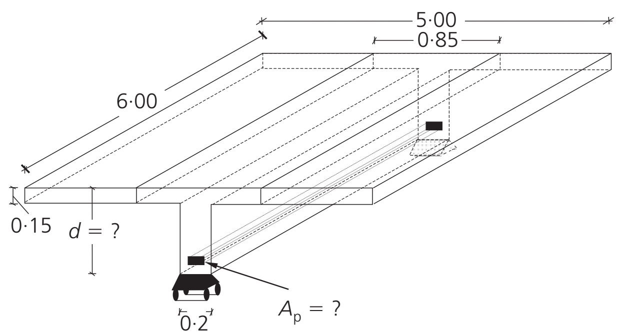

Figure 4. Structural configuration

Proposals have been made to improve the ductility of beams with FRP by adding confinement reinforcement to the compression zone (Leung, 2000; Mikami *et al.*, 1989), but there is little benefit for reinforced concrete since the curvatures at failure are very large and the compression area after cracking is small, so the addition of confinement reinforcement would have little effect.

Deflections are assumed to be limited to span/250 unless otherwise stated while the concrete cover is taken as 50 mm for FRPs

Material	Form	Strength: N/mm²	Elastic modulus: kN/mm²	Snapping strain	Partial safety factor	B[a]
GFRP	Pultruded rod	1200	40	0·030	1·3	0·101
AFRP-Fibra	Braided rod	1480	68	0·022	1·3	0·069
AFRP-Technora	Pultruded rod	1900	56	0·034	1·3	0·053
CFRP	Pultruded rod	2200	140	0·012	1·3	0·016
Parafil	Parallel-lay rope	1900	120	0·016	1·3	0·069
Steel rebar	Rod	460	210	0·1	1·15	—
Steel tendon	7-wire strand	1700	200	0·1	1·15	—

[a] Determined by fitting on data shown in Giannopoulos and Burgoyne (2009) and Yamaguchi *et al.* (1998).

Table 1. Material properties

Structure properties	
Desired lifetime: years	120
Span: m	6
Beam web width: m	0·25
Slab depth: m	0·15
Slab width: m	5
Beam top flange effective width: m	0·85
Cover: mm	50 (FRP) 75 (steel)
Loading properties	
Slab's short-term live load: kN/m^2	1·0
Slab's long-term live load: kN/m^2	1·0
Partial dead load safety factor (ultimate)	1·4
Partial live load safety factor (ultimate)	1·6
Partial dead, live load safety factor (working)	1·0
Concrete properties	
Strength: N/mm^2	30
Ultimate strain	0·0035
Partial safety factor	1·5

Table 3. Parameters for reinforced beam comparisons

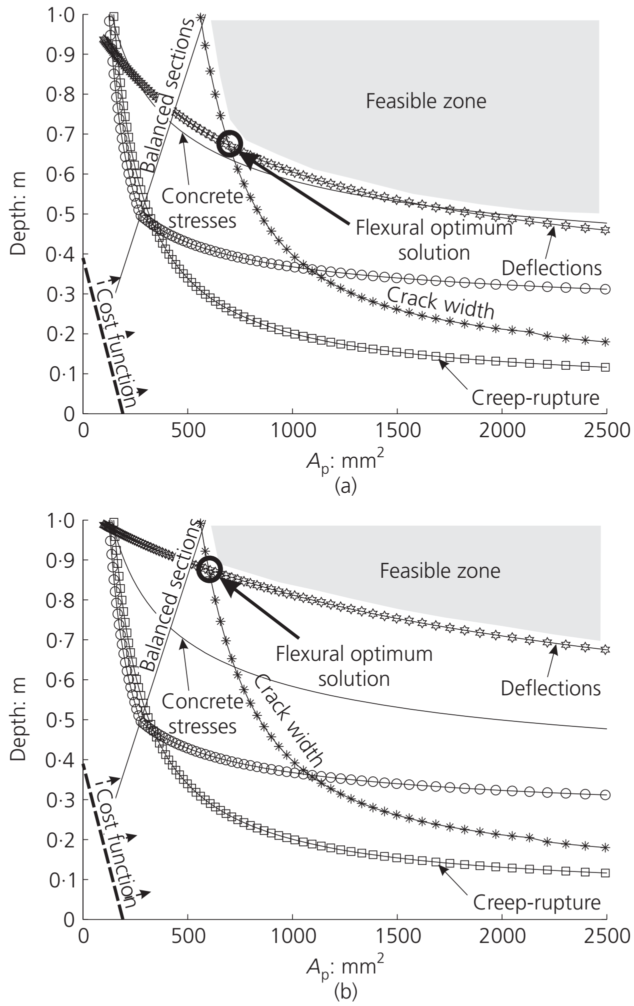

Figure 5. Technora reinforced beam with deflection limits: (a) span/180; (b) span/480

and 75 mm for steel owing to durability concerns. The crack widths are limited to 0·3 mm for all FRPs and 0·2 mm for steel. The concrete compression stress under service loads is limited to 40% of the characteristic concrete strength. Stirrups are provided according to standard practice and are assumed to be made from the same material as the flexural reinforcement.

Deflection limit and material

Varying the deflection limit from the normal span/250 shows how the governing criteria can change. Deflection limits were imposed from span/180 to span/480. All the other values were taken as in Table 1. Figure 5 shows the effect on a beam reinforced with relatively flexible Technora bars. In Figure 5(a) the most relaxed deflection limit is imposed. The optimal solution is found to lie at the intersection of the crack width and deflection constraints. On the other hand, in Figure 5(b) the most strict deflection limit (span/480) is applied; the deflection constraint moves higher, reducing beam deflections, while all the other constraints remain unchanged. Consequently, the optimal solution is also at the intersection between crack width and deflections constraints.

For steel-reinforced beams the ultimate load condition governs except when the most severe deflection constraint is applied. However, for the FRP-reinforced beams, owing to their much lower modulus, the optimum solution is almost invariably governed by deflection constraints at the working load. For relaxed deflection limits and low elastic modulus FRPs such as glass and Technora, the optimal solution lies at the intersection with the crack width limit, whereas for stiffer FRPs or tighter deflection conditions, the optimum condition is usually at the intersection of the deflection and balanced-section constraints.

In Figure 6, cost ratios relative to the cost of the steel-reinforced beams are shown. Total costs include formwork, concrete, flexural and shear reinforcements costs. The figure shows that GFRP reinforcement is only marginally more expensive than steel-reinforced sections, although of course with much deeper sections. The use of the higher-modulus FRPs seems never to be cost-effective for reinforced sections, and in general applying more severe deflection constraints increases the cost ratio.

Sensitivity to price reduction

It has long been assumed that FRP reinforcement would become more economic as the price dropped by the economy of scale theory (Varian, 1999). Figure 7 shows that, because the optimal design lies at a sharp vertex of the feasible zone, reducing the cost of the reinforcement (in this case, FiBRA) by 40% does not alter the optimal design, although it does, of course, reduce the cost of the section. The cost of the reinforcement needs to be almost as cheap as steel, on the basis of a cost per unit volume,

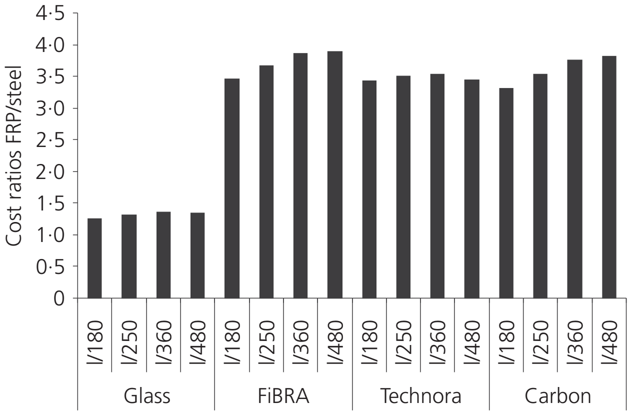

Figure 6. Cost of RC beams with different materials and different deflection limits

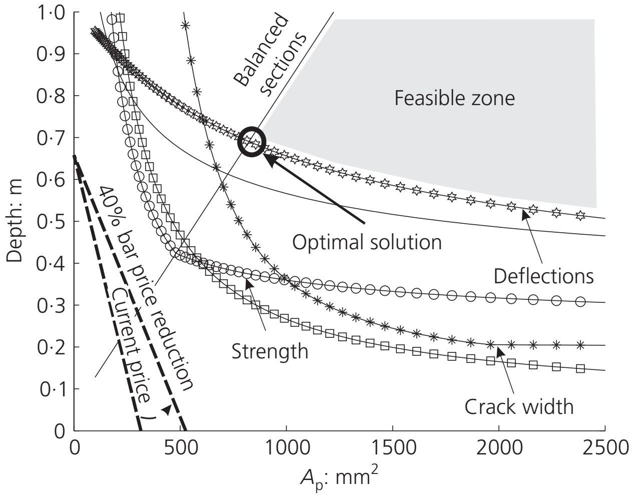

Figure 7. Effect of reducing cost of FRP (Fibra) by 40%

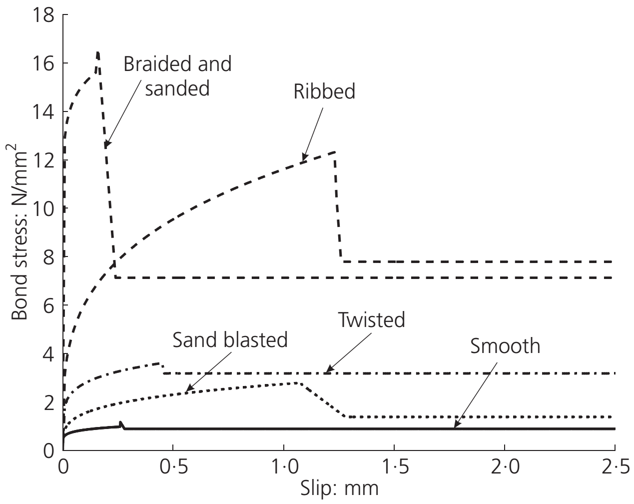

Figure 8. Bond–slip curves (Cosenza *et al.*, 1997)

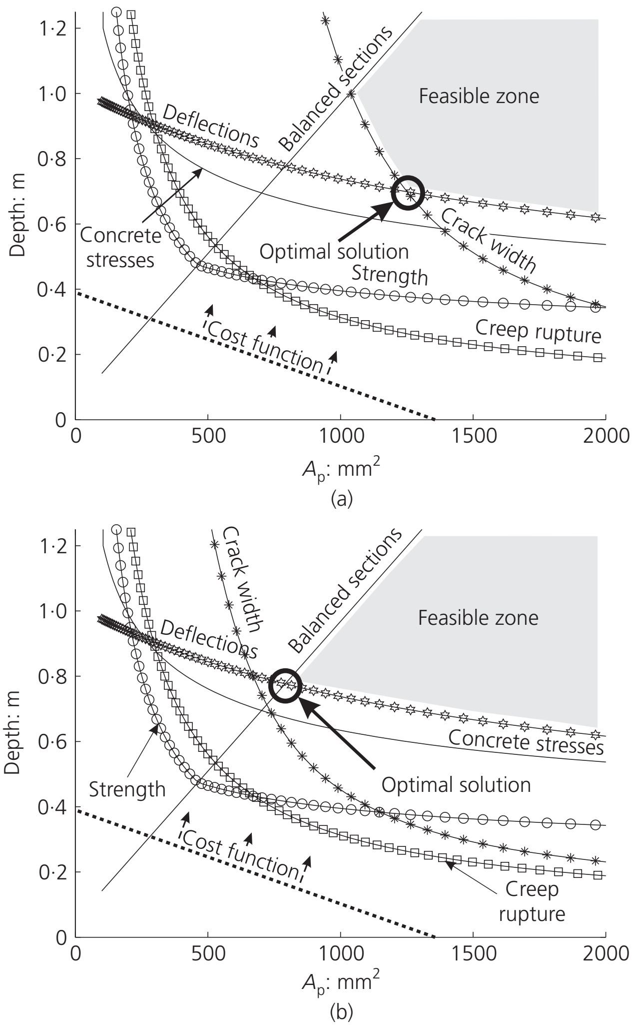

Figure 9. Design curves for GFRP bars: (a) smooth; (b) braided and indented

before there is any effect on the position of optimal solution in the diagram.

Bond

Bond strength does not normally affect the design of a cross-section, provided there is enough to grip the rebar at its ends. However, it can have an effect on the crack widths, and because FRPs have low stiffness, those limits can be critical. Manufacturers have produced bars with various surface characteristics with a view to improving bond; representative bond–slip curves, which are assumed to apply to all types of FRP, are shown in Figure 8 (Cosenza *et al.*, 1997).

Two d–A_p diagrams are shown. Figure 9(a) shows the effect of having a smooth surface, where the crack-width criterion dominates, while Figure 9(b) shows the result for a beam with braided and indented GFRP bars, which bond very strongly to concrete. As a result, the crack width constraint moves to the left on the figure and no longer governs. The best solution is then found at the deflection and balanced-section crossing point.

The effects of the different types of bond are shown in Figure 10. For beams with low elastic modulus fibres, such as glass and aramid-Technora, low bond strength is a disadvantage, whereas stiffer bars, such as FiBRA and CFRP are not affected by the crack width criterion.

Partial material safety factor

Lack of knowledge on durability and long-term behaviour of FRPs has led to various proposals on partial material safety factors (*fib*, 2003). To assess the effect of the partial material safety factor on the optimal solution, values between 1·3 and 2·0 were studied and the optimal solutions were found in each case. The partial material safety factors will only affect the ultimate condition constraints; unity safety factors are assumed in service conditions. However, since the balanced section condition is there to prevent the bar snapping, increasing the safety factor makes this constraint much more severe.

The balanced-section constraint rotates clockwise on the depth plotted against bar area diagram and the ultimate constraint moves upwards as shown in Figure 11, which results in a substantial increase in total cost when the safety factor is raised. As the deflection constraint still governs, more bars have to be provided to prevent bar snapping at failure but the beam can be less deep.

Concrete strength

Owing to FRP's low elastic modulus, the results up to this point have shown that the deflection constraint usually governs the optimal design solution. The use of stiffer high-strength concrete has been proposed to limit the problem of excessive deflections of structures reinforced with these materials (Nanni, 1993).

Analyses have been performed to assess the effect of high-strength concrete in FRP-reinforced concrete design. The deflection constraint does indeed yield lower depths but this is balanced by a clockwise rotation of the balanced-section line on the d–A_p figure; more bars are needed to crush the stronger concrete. In general, the latter effect more than offsets the cost reduction owing to the stiffer concrete and there is no benefit in using stronger concrete.

Flexural against total costs

The d–A_p diagrams give flexural optimum results by inspection, which for expensive FRPs are normally located at the intersection between the deflection and the balanced-section conditions. The total cost has to include the shear reinforcement as well and these can be determined from the flexural design. The optimal beam depths for low elastic modulus FRPs are normally high to avoid extensive deflections; increasing beam depth enhances shear capacity and fewer stirrups may be needed. In certain circumstances, however, a default minimum amount of shear links have to be provided; consequently stirrup volume may increase.

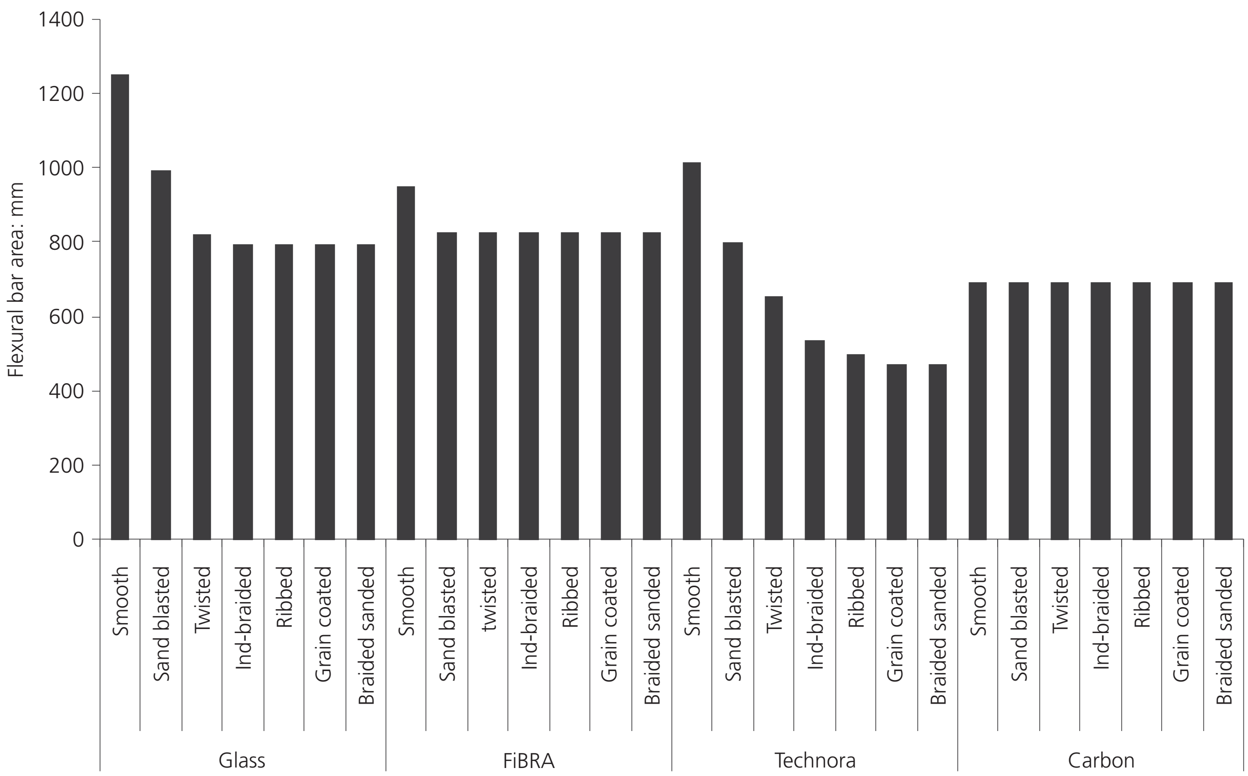

Figure 10. Effect of bond on amount of FRP needed

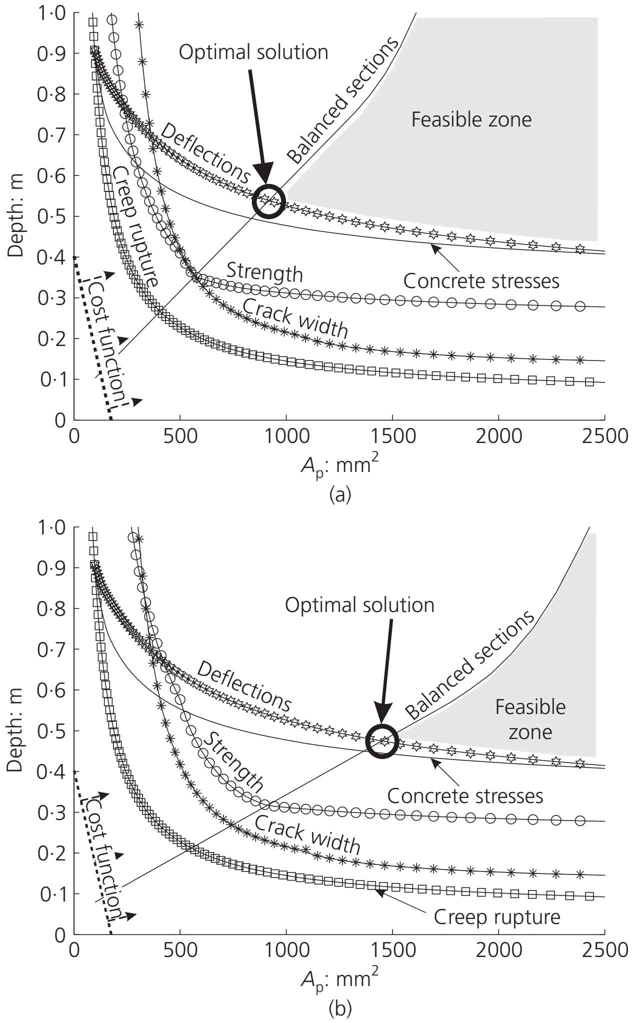

Figure 11. Effect of varying partial material safety factor for CFRP-reinforced beams: (a) $\gamma = 1{\cdot}3$; (b) $\gamma = 2{\cdot}0$

When stirrup volume increases with beam depth, the total cost function reduces its slope on the d–A_p diagram and the optimal solution may lie at a reduced beam depth. The shear demand for the beams reinforced with FRP stirrups was determined by assuming truss analogy and stress limitation on the FRP stirrups (Guadagnini *et al.*, 2003, 2006). Studies were carried out to see the effect of this on the amount of FRP provided, but it was found that this would only be significant if FRP stirrups were many times more expensive than the cost of straight FRP rebar. This was beyond the scope of this study since it depends on the methods adopted to produce the links.

Case study 2. Determinate prestressed concrete

Prestressed concrete ought to be a logical application for FRPs, and the initial cost model can also be used to identify ways in which they can best be used in determinate prestressed concrete design.

It has also been identified that elements prestressed with FRP can benefit from confinement (Burgoyne, 2001) because this provides ductility to the compression zone of the concrete. It is assumed here that the FRP prestressed beam's top flange can be confined with 100 mm diameter AFRP spirals (Leung and Burgoyne, 2005). Spirals are placed in regions where the moment is highest, and thus where crushing is more likely. The spiral pitch is assumed to be 100 mm, which is the minimum needed to ensure that the spirals are effective in ensuring that concrete does not fail explosively. As moment redistribution is not required, denser confinement spacing is not needed.

The structure used for comparison purposes is similar to the reinforced structure considered above, but with a 12 m span and an I-shaped cross-section. Various inputs assumed in the analysis, such as structural and material properties, as well as design limits, are summarised in Table 4.

The prestressing tendons are initially prestressed to 60% of their ultimate limit strength for steel and CFRP tendon. A lower value is chosen for FiBRA, Technora and Parafil tendons owing to creep-rupture concerns (Table 4). Concrete creep, shrinkage and tendon relaxation are also taken into account.

Bonding to concrete

It is not clear whether FRP tendons should be connected to concrete (Abdelrehman and Rizkalla, 1997; Burgoyne, 1993). Bond conditions have a considerable influence on tendon effectiveness and cost (Lees and Burgoyne, 1999). The method described there was applied to determine the effect of bond on the final optimal solution. Three different scenarios were assumed: one with the tendons fully bonded to the concrete, one fully unbonded, while the last has partially bonded tendons, similar to those tested by Lees and Burgoyne (1999). This reduces the local strain that is attracted to the tendon, thus reducing the likelihood that the tendon will snap.

When fully bonded conditions do not exist, the plane-section-remains-plane assumption no longer applies as the tendon sees lower strains than the concrete. The effect depends on tendon prestress, tendon profile, tendon length/static depth and loading type (Janney *et al.*, 1956). To allow for these effects, strain reduction factors (Ω) are introduced for the uncracked as well as for the cracked plane section analysis (Balafas, 2003; Naaman and Alkhairi, 1992).

Strain reduction factors do not exist in the literature for partially bonded prestressed beams. A value for Ω halfway between unity and that determined for the unbonded tendons is assumed to represent strain sensitivity in partially bonded beam.

The plot shown in Figure 3(a) shows that for steel tendons the optimal solution was governed by concrete tensile stresses at the working load and, owing to the cost function slope, it was located towards higher tendon areas and away from the balanced-sections constraint.

Structure properties	
Desired lifetime: years	120
Span: m	15
Beam web width: m	0·30
Beam top flange width: m	1·5
Beam bottom flange width: m	0·55
Beam bottom flange depth: m	0·2
Slab depth: m	0·15
Slab width: m	5
Cover: mm	100
Loading properties	
Slab uniform live load: kN/m^2	2·0
Slab uniform superimposed dead load: kN/m^2	1·0
Partial dead load safety factor (ultimate)	1·4
Partial superimposed dead load safety factor (ultimate)	1·2
Partial live load safety factor (ultimate)	1·6
Partial dead, live load safety factor (working)	1·0
Concrete properties	
Strength: N/mm^2	60
Confinement spacing: mm	100
Partial safety factor	1·5
Initial prestressing ($t = 0$)	
Steel: %	60
CFRP: %	60
AFRP (FiBRA and Technora), Parafil rope: %	55
Design limits	
Deflections: m	Span/250
Transfer stress limits: N/mm^2	−1 (tension), 18 (compression)
Working stress limits: N/mm^2	0, 25 (compression)

Table 4. Parameters for prestressed beam comparisons

In contrast, FRP tendons are expensive; thus the cost function is steeper on the d–A_p diagram. Flexural optimal solutions for the FRP prestressed beams are almost always located where the concrete tensile stress limits and the balanced-section conditions intersect. Typical plots for a beam with bonded, unbonded, and partially bonded FiBRA tendons are shown in Figure 12.

The differences between the three cases are clear. Most of the constraints do not change significantly, but the balanced section constraint is much more severe for the fully bonded case. The ultimate strength, creep rupture and deflection constraints shift to lower section depths and tendon areas as the bond increases, while the transfer constraints are the same for both cases. For all of these reasons, bonded beams are always more expensive than those with unbonded tendons.

As the cheapest way to use FRPs in prestressed concrete design is by debonding them from concrete, all the FRP beams examined in the sections below are unbonded, unless stated otherwise.

Price reduction

When designing beams with FRP rebar, the optimal design was at a sharp vertex of the feasible region, and very large changes in cost of FRP would be needed to alter the optimum. However, the shape of the feasible zone with prestressed beams means that, although it still occurs at a vertex, one of the lines at that intersection has a similar slope to the cost function. Thus, changes to the cost of the material would lead to alterations in the optimal design. These effects are illustrated in Figure 13(a) and Figure 13(b). A 40% reduction in the cost of CFRP would not alter the optimal solution – it would remain at the vertex, but for Technora a 40% reduction in price would move the optimal solution to a lower depth and higher tendon area (and thus higher prestress). It is still clear, however, that significant price changes

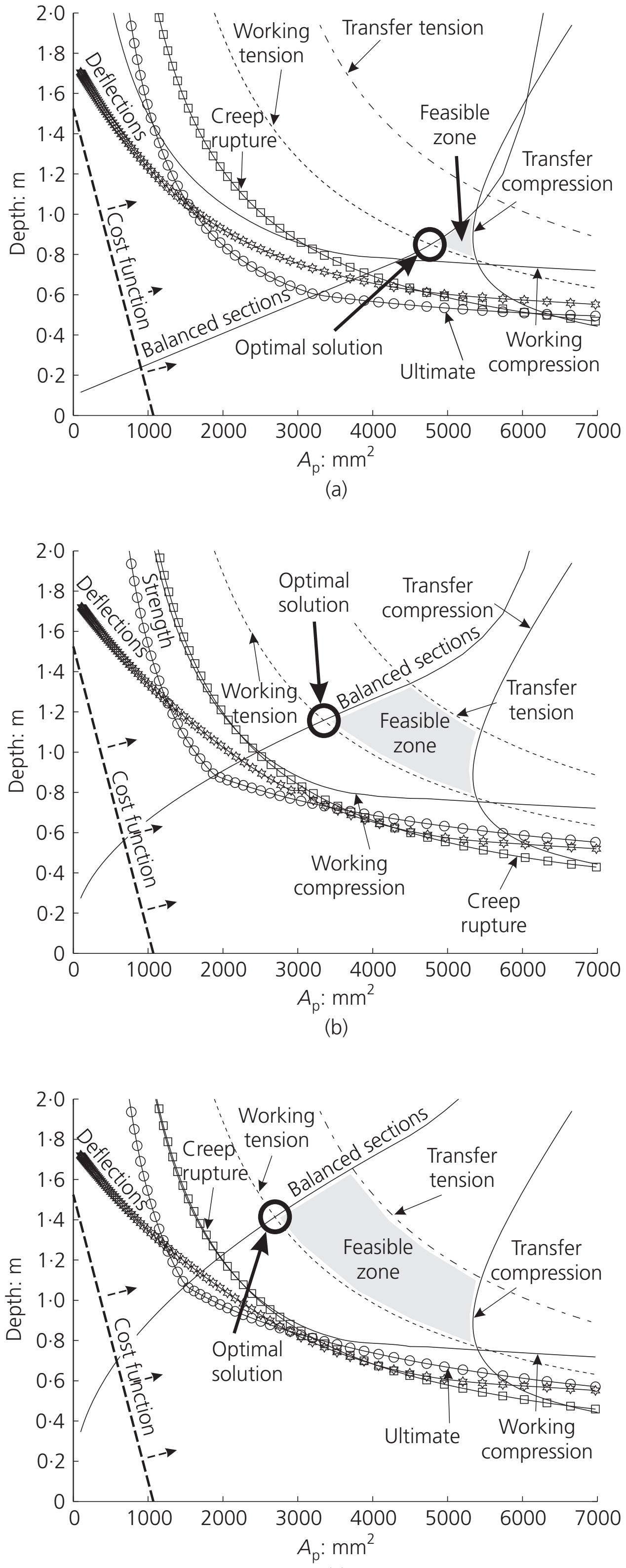

Figure 12. Prestressed beams with FiBRA tendons: (a) fully bonded; (b) partially bonded; (c) unbonded

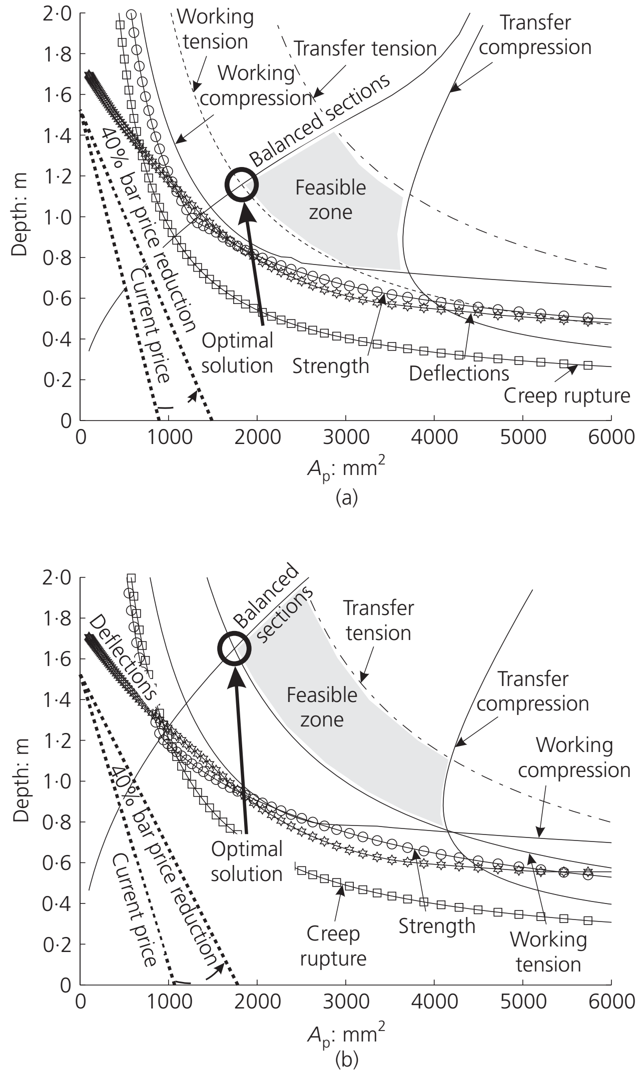

Figure 13. Prestressed beam. Effect of price on: (a) CFRP; (b) Technora

would be needed before the cost of structures with FRP matched the initial cost of structures with steel tendons.

Concrete strength – deflection limits

Concrete strength has little effect on the total cost. When the concrete strength increases, more tendon area is needed to eliminate the tendon snapping mode of failure. Thus the balanced-section constraint rotates to require a greater tendon area, but this is partly offset by the better shear capacity of stronger concrete.

The imposition of stricter deflection limits does not affect the optimal solution for prestressed concrete since pre-straining flexible FRPs eliminates the problem of deflections, as the concrete remains uncracked. Even for extreme deflection limits as much as span/480, the same criteria (tensile stresses in the concrete at the working load and balanced-section constraints) still govern.

Case study 3. Indeterminate prestressed concrete

The design of indeterminate prestressed concrete structures differs from the determinate beams as more constraints come into play. The amount of prestress has to be satisfactory for both positive and negative moments, which have an effect both on the amount of prestress and the depth of the beam. It is also necessary to ensure that the beam has adequate ductility to take benefit from the moment redistribution that can occur in such beams. It is often assumed that beams with FRP are less ductile than beams with steel, but the large strain capacity of FRPs usually means that large rotations can occur as the concrete cracks.

A continuous three-span prestressed concrete beam supporting a loaded slab is assumed. Structural and section dimensions, as well as loading properties, are shown in Table 5. Secondary moments are not considered since these would require the complete cable profile to be calculated which is beyond the scope of this paper.

New design constraints were introduced using the theory of Low (1982): P_2 limits which ensure that tendon eccentricities fit in the beam depth and P_3 limits which ensure that concordant tendon profiles exist in allowable tendon eccentricities; detailed description of those limits can be found elsewhere (Balafas, 2003).

In particular, for continuous beams prestressed with brittle FRPs, provision of confinement in the compression zone is essential (Burgoyne and Leung, 2010). The structure has to behave non-linearly so that moment redistribution takes place and failure does not occur when one of the points on the structure fails. Non-linear behaviour is also needed for design calculations to be justified through the safe theorem of plasticity.

The regions where concrete is likely to fail in compression are confined with AFRP spirals similar to those tested by Burgoyne and Leung (2010). The spirals are placed in the top flange in sagging moment regions (mid-span) and in the bottom flange in hogging moment regions. The length over which they are extended is chosen to be 70% of the span's length for top flange confinement and 30% of the span for the bottom flange.

Structure properties	
Desired lifetime: years	120
Spans: m	15–20–15
Beam web width: m	0·3
Beam top flange width: m	1·5
Beam bottom flange width: m	0·9
Beam bottom flange depth: m	0·2
Slab depth: m	0·2
Slab width: m	5
Cover: mm	100
Loading properties	
Slab uniform live load: kN/m^2	2·0
Slab uniform superimposed dead load: kN/m^2	1·0

Table 5. Parameters for continuous prestressed beam comparisons

Four different spiral pitches were chosen: 100, 50, 35 and 10 mm. A moment redistribution of 0, 5, 10 and 20% is also assumed to occur respectively before the structure fails. There are not yet sufficient data to allow an accurate calculation of the moment redistribution extent according to the spiral spacing provision. No redistribution is assumed to take place at 100 mm spiral spacing, as this is equal to spiral diameter and tests have shown that at this spacing concrete fails in a gentler manner, but with limited non-linearity.

When the confinement is increased, the concrete failure strain increases and thus the danger of snapping of tendon before concrete crushing is increased. This can be seen on Figure 14

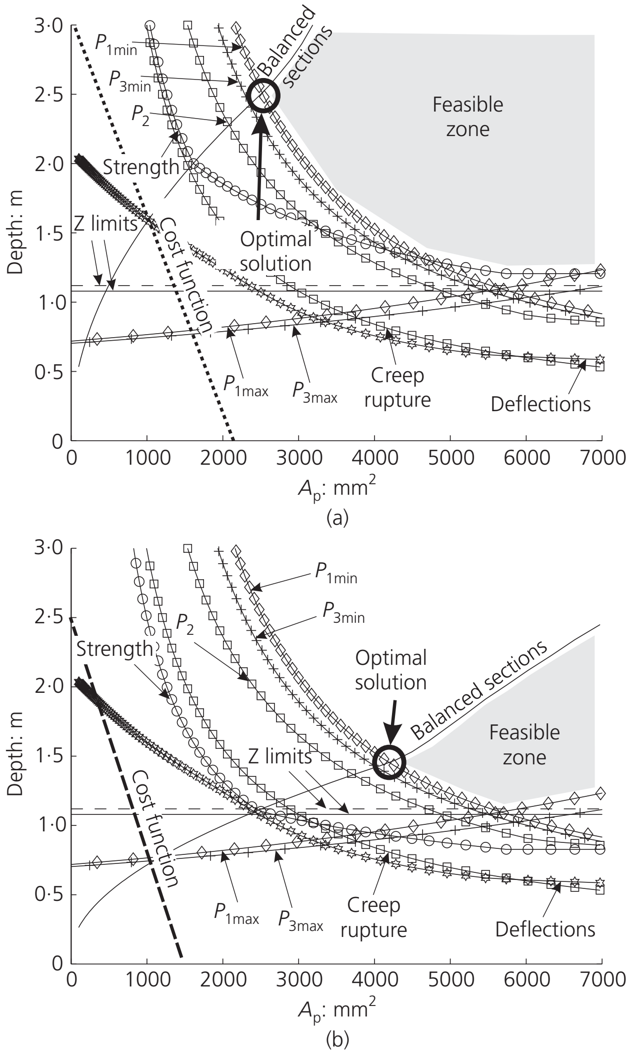

Figure 14. Indeterminate prestressed beam. Technora spirals: (a) 100 mm pitch; (b) 10 mm pitch

where two d–A_p diagrams are plotted for beams prestressed with unbonded Parafil tendons with 100 mm and 10 mm spiral pitch. The balanced-section constraint moves to greater tendon areas when confinement is increased. In addition, the ultimate constraint relaxes to lower section depths and tendon areas as redistribution takes place. The net effect is that the tendon area has to increase with a corresponding increase in the optimal cost.

It can be concluded that there is not much benefit in providing confinement in the compression zone since it can change the mode of failure, threaten the safety of the structure and increase cost considerably. Further research is needed in this area.

Conclusions

A method has been introduced that allows the optimal design, and hence initial costs, of concrete beams reinforced and prestressed with FRPs to be studied. Beams with steel and FRP reinforcements were optimised and comparisons were made. Some conclusions can be drawn from the analytical results.

For the reinforced structures, the following are observed.

(*a*) The serviceability limit state condition, in most cases deflections or crack widths, govern the design due to the relatively high flexibility of FRP as concrete section reinforcement.
(*b*) As the FRP-snapping mode of failure has to be eliminated, the optimum solution will normally be at the intersection of the above condition and the balanced-section constraints.
(*c*) For the most flexible FRP bars (GFRP and Technora-AFRP) with poor bond properties (sandblasted or twisted), crack widths may be wide under service loads and these will govern for aesthetic reasons. For stiffer bars (AFRP-FiBRA and CFRP) the deflection criterion governs.
(*d*) Using stronger concrete to diminish the excessive deflections does not seem to solve the problem. The stronger concrete is harder to crush and more bars are needed for that purpose. As stronger concrete is more expensive a cost increase was observed.
(*e*) Beams with FRP reinforcement are usually deeper than their steel-reinforced counterparts and have higher deflections, but use less reinforcing material because it is stronger.
(*f*) As the optimal design is at a vertex of the feasible region, small changes to the design do not reduce the cost. Beams with GFRP are slightly more expensive than beams with steel but it is unlikely that beams designed with stiffer FRP reinforcement will ever be economic on a first-cost basis.

For simply supported and continuous prestressed concrete structures the following conclusions can be made.

(*a*) Optimum solutions are governed by the tension stress limits in the cross-section under working load conditions and the balanced-section constraint, as the tendon snapping mode has to be prevented.
(*b*) In contrast to steel-prestressed bridges, less tendon bond to concrete produces cheaper solutions. When tendons are bonded they tend to fail by snapping and the designer will be forced to use more FRPs.
(*c*) Spiral provision to enhance concrete plasticity triggers tendon snapping and more flexural bars are needed to avoid this mode of failure.
(*d*) For bonded FRP tendons higher prestressing does not necessarily mean reduced cost.
(*e*) Designs with unbonded prestressing tendons are the most likely application for economic use of FRP in concrete.

For reinforced and prestressed structures, the ultimate moment capacity constraint is very unlikely to be one of the governing constraints and the optimum structural dimensions remain the same even for the most optimistic future FRP price predictions. On the other hand, the balanced-section constraint proves to be a governing constraint in most cases. Hence, the design calculations should

(*a*) determine the material volumes for a balanced section and
(*b*) check
  (*i*) deflections for reinforced concrete designs or
  (*ii*) stress limits in prestressed concrete design.

The outcome will then be very close to optimal in terms of cost.

From the above study it is clear that the initial cost of FRP-reinforced or prestressed concrete structures is higher than those with steel, which explains why there are so few commercial applications of FRP to date. These additional costs cannot be justified unless life-cycle costs are taken into account. Whole-life costs for bridges can be enormous, especially if the user's costs are taken into account as well as the owner's, and if they are ignored, the cost estimation is far from being complete (Balafas, 2003; Balafas and Burgoyne, 2004).

Acknowledgement

The EU-TMR network ConFibrecrete is gratefully acknowledged for funding this work.

REFERENCES

Abdelrehman AA and Rizkalla SH (1997) Serviceability of concrete beams prestressed by carbon-fibre-reinforced-plastics bars. *ACI Structural Journal* **94(4)**: 447–457.
Al-Salloum YA and Siddiqi GH (1994) Cost optimum design of reinforced concrete beams. *ACI: Structural Journal* **91(6)**: 647–655.
Balafas I (2003) *Fibre-Reinforced-Polymers vs Steel in Concrete Bridges: Structural Design and Economic Viability*. PhD thesis, University of Cambridge, UK.
Balafas I and Burgoyne CJ (2004) Economic viability of structures with FRP reinforcement or prestress. *Proceedings of the 4th Conference on Advanced Composite Materials in Bridges and Structures, Calgary, Canada*, paper 186.

Burgoyne CJ (1993) Should FRP be bonded to concrete? In *Non-Metallic (FRP) Reinforcement for Concrete Structures, FRPRCS-1, SP138* (Nanni A and Dolan CW (eds)). American Concrete Institute, Farmington Hills, MI, USA, pp. 367–380.

Burgoyne CJ (2001) Rational use of advanced composites in concrete. *Proceedings of the Institution of Civil Engineers – Structures and Buildings* **146(3)**: 253–262, http://dx.doi.org/10.1680/stbu.2001.146.3.253.

Burgoyne CJ and Leung HY (2010) Test on prestressed concrete beam with AFRP spiral confinement and external aramid tendons. In *Proceedings of Antoine E. Naaman Symposium – Four Decades of Progress in Prestressed Concrete, Fiber Reinforced Concrete, and Thin Laminate Composites*, *SP272-04*. American Concrete Institute, Farmington Hills, MI, USA, vol. 272, pp. 69–86.

Cosenza E, Manfredi G and Realfonzo R (1997) Behavior and modelling of bond of FRP rebars to concrete. *ASCE Journal of Composites for Construction* **1(2)**: 40–51.

fib (2003) *fib-TG-9.3*. Chapter 3: Reinforced Concrete. *fib* Model-Code on Fibre Reinforced Polymer Reinforcement (Riga Draft). CEB Committee TG9.3. Fédération Internationale du Béton, Lausanne, Switzerland.

Fickelhorn M (1990) Editorial. *Materials and Structures, RILEM* **23(137)**: 317.

Giannopoulos IP and Burgoyne CJ (2009) Stress limits for aramid fibres. *Proceedings of the Institution of Civil Engineers – Structures and Buildings* **162(4)**: 221–232, http://dx.doi.org/10.1680/stbu.2009.162.4.221.

Guadagnini M, Pilakoutas K and Waldron P (2003) Shear performance of FRP reinforced concrete beams. *Journal of Reinforced Plastics and Composites* **22(15)**: 1389–1407.

Guadagnini M, Pilakoutas K and Waldron P (2006) Shear resistance of FRP RC beams: experimental study. *Journal of Composites for Construction, ASCE* **10(6)**: 464–473.

Hambly EC (1991) *Bridge Deck Behaviour*, 2nd edn. Taylor & Francis, Abingdon, UK.

Janney JR, Hognestad E and McHenry D (1956) Ultimate flexural strength of prestressed and conventionally reinforced concrete beams. *American Concrete Institute* **27(6)**: 601–620.

Lees JM and Burgoyne CJ (1999) Experimental study of the influence of bond on the flexural behaviour of concrete beams pre-tensioned with aramid fibre reinforced plastics. *ACI Structural Journal* **96(3)**: 377–385.

Leung HY (2000) *Study of Concrete Confined with Aramid Spirals*. PhD thesis, University of Cambridge, UK.

Leung HY and Burgoyne CJ (2005) The uniaxial stress–strain relationship of spirally-confined concrete. *ACI Materials Journal* **102(6)**: 445–453.

Low AM (1982) The preliminary design of prestressed concrete viaducts. *Proceedings of the Institution of Civil Engineers* **73(2)**: 351–364, http://dx.doi.org/10.1680/iicep.1982.1705.

Makhtouf HM, Abmadi BH and Al-Jabal J (1991) Preventing reinforced concrete deterioration in the Arabian Gulf. *Concrete International* **13(5)**: 65–67.

Mikami H, Katoh M, Takeuchi H and Tamura T (1989) Flexural and shear behaviour of RC beams reinforced with braided FRP rods in spiral shape. *Transaction of the Japan Concrete Institute* **11(1)**: 119–206.

Naaman AE and Alkhairi FM (1992) Stress at ultimate post-tensioned tendons: Part 2 – proposed methodology. *American Concrete Institute: Structural Journal* **88(6)**: 683–692.

Nanni A (1993) Flexural behaviour and design of RC members using FRP reinforcement. *ASCE, Journal of Structural Engineering* **119(11)**: 3344–3359.

Varian HR (1999) *Intermediate Microeconomics*, 5th edn. W. W. Norton, London, UK.

Yamaguchi T, Nishimura T and Uomoto T (1998) Creep model of FRP rods based on fiber damaging rate. *Proceedings of the 1st International Conference (CDCC 1998), Durability of Fibre Reinforced Polymer Composites for Construction* (Benmokrane B and Rahman H (eds)), pp. 427–438.